Coarse-grained computations of demixing in dense gas-fluidized beds

Sung Joon Moon, S. Sundaresan, and I. G. Kevrekidis*
Department of Chemical Engineering & Program in Applied and Computational Mathematics, Princeton University, Princeton, New Jersey 08544, USA

(Received 6 November 2006; revised manuscript received 19 January 2007; published 29 May 2007)

We use an "equation-free," coarse-grained computational approach to accelerate molecular dynamics-based computations of demixing (segregation) of dissimilar particles subject to an upward gas flow (gas-fluidized beds). We explore the coarse-grained dynamics of these phenomena in gently fluidized beds of solid mixtures of different densities, typically a slow process for which reasonable continuum models are currently unavailable.

DOI: 10.1103/PhysRevE.75.051309 PACS number(s): 45.70.Mg, 47.11.St, 47.61.Jd

I. INTRODUCTION

Particulate flows, even for experimental systems of small size (~10 cm), consist of a very large number of discrete dissipative particles. Molecular dynamics (MD) simulations often serve as a quantitative modeling tool for such flows; however, such simulations for realistically large temporal and/or spatial scale problems are challenging, even with modern computers.

In most particulate flows, relevant spatial and temporal scales are much larger than those of individual particles, and the development of macroscopic, coarse-grained models is one of the outstanding issues in the statistical mechanics of such flows. In this paper, we refer to the MD simulation as the microscopic (or detailed) model, and to the extraction of lower-dimensional, hydrodynamic-level descriptions as *coarse-graining*. Navier-Stokes-like continuum models, based on the kinetic theory of granular materials (see Refs. [1,2] and references therein), have been developed by many authors; however, *quantitative* coarse-grained models for realistic particles (accounting for frictional interactions, heterogeneity among particles, and/or other interparticle forces, such as van der Waals forces) in many regimes of practical interest (e.g., dense and/or cohesive particulate flows where enduring contacts between particles occur) are currently unavailable. Our approach aims at enabling MD-level simulations to perform coarse-grained modeling tasks precisely in cases where explicit coarse-grained models are unavailable.

We will illustrate our approach using well-known phenomena for which the derivation of coarse-grained models is still in flux; mixing and demixing (segregation) can occur when dissimilar particle mixtures of different sizes and/or densities are subject to a strong enough upward fluid flow [3]. A few different continuum models, some more phenomenological and other more rigorous, have been proposed [4,5]. Such models often reproduce the phenomena in a qualitatively correct manner; however, quantitative agreement is generally elusive [5]. Furthermore, kinetic theory-based continuum models for binary mixtures are much more complicated than those for uniform particles, and numerical simulation becomes more time-consuming (e.g., by an order of magnitude in Ref. [5]). In the absence of a quantitative coarse-grained model, accelerating the computation using (quantitative) microscopic models becomes vitally important.

The objective of this paper is to demonstrate a multiscale computational approach, the so-called "equation-free" coarse-grained approach, enabling accelerated integration of MD-based microscopic simulations of dense particulate flows. This recently developed approach has been applied to a range of science and engineering problems where coarse-grained model is believed to exist, yet only a microscopic, detailed model is available [6,7]. In this approach, quantities necessary for traditional continuum numerical analysis are *estimated* from short bursts of microscopic simulation (rather than from evaluating explicit coarse-grained equation formulas). As a result, coarse-grained computations are done without ever using their governing equations; the approach is therefore called "equation-free."

Our paper is organized as follows: An MD-based detailed model for gas-fluidized beds of particle mixtures is described in Sec. II. We start by presenting some demixing results obtained by (brute-force, highly time-consuming) direct simulations, and then identify possible coarse-grained variables that can be used for closures of a hydrodynamic-like coarse-grained model (Sec. III). We explain ideas and procedures of equation-free computation in Sec. IV, and follow this approach to efficiently integrate demixing simulations using two different levels of coarse-graining (Secs. IV B and IV C). The paper is concluded in Sec. V.

II. DETAILED, FINE-SCALE MODEL

Particles are assumed to be uniform-sized soft spheres (which can have different mass), whose contact force is modeled following Cundall and Strack [8], decomposing the interacting force into the normal and tangential directions relative to the displacement vector between the objects at contact, $\mathbf{F}_{\text{cont}}=(\mathbf{F}_n,\mathbf{F}_s)$ [8]:

$$\mathbf{F}_n = (k_n\Delta_n - \gamma_n v_n)\hat{\mathbf{n}}, \tag{1}$$

$$\mathbf{F}_s = -\operatorname{sgn}(v_s)\times\min(k_t\delta s, \mu|\mathbf{F}_n|)\hat{\mathbf{s}}, \tag{2}$$

where k_n is the (Hookean) spring stiffness in the normal direction; Δ_n is the amount of overlap; γ_n is the damping co-

*Electronic address: yannis@princeton.edu

efficient (determining the coefficient of restitution e); v_n is the normal component of the relative velocity at contact; $\hat{\mathbf{n}}$ is the unit vector in the normal direction at contact pointing outward from the particle center; v_s is the tangential component of the relative velocity at contact; k_t is the tangential spring stiffness that is related to k_n by the Poisson's ratio of the material ν_P [$k_t=2k_n(1-\nu_P)/(2-\nu_P)$; a typical value of 0.3 is used for ν_P]; δs is the magnitude of tangential displacement from the initial contact; μ is the coefficient of friction; $\hat{\mathbf{s}}$ is the unit vector in the tangential direction at contact.

The gas phase hydrodynamics is accounted for in a volume-averaged way [9,10]. The same type of model has been used to study size difference-driven demixing [11]; here we consider *density-driven* demixing. The equation of motion for each particle is

$$m_p \frac{d\mathbf{v}_p}{dt} = m_p \mathbf{g} + \mathbf{F}_{\text{cont}} + \frac{V_p}{\phi}\beta(\phi)(\mathbf{u}_g - \mathbf{v}_p) - V_p \nabla p, \quad (3)$$

where m_p and $\mathbf{v}_p$ are individual particle mass and velocity, respectively. The right-hand side includes various forces acting on the particle, the last two terms arising from the gas-solid two-way coupling; the total force acting on the particles due to the fluid is commonly partitioned into the local drag part and the effective buoyant part [10], as was done here. The first term is the body force due to gravity, where $\mathbf{g}$ is the gravitational acceleration, and the second term is the aforementioned contact force. The third term accounts for the drag force, where β is the interphase momentum transfer coefficient [12,13], ϕ is the local particle phase volume fraction, $\mathbf{u}_g$ is the local-average gas phase velocity, and V_p is the individual particle volume. The last term accounts for the hydrodynamic force due to the gradually varying part of the pressure field, where p is the local-average gas phase pressure.

We deliberately choose demixing occurring in narrow beds (cross sectional area of $15d_p \times 15d_p$ with periodic boundary conditions for both lateral directions, where d_p is the particle diameter) as a test problem; for this problem size brute-force computations with the detailed model are still feasible, and can then be used to critically test and validate the coarse-grained computations presented below. These are quasi-1D flows, where the coarse-grained gas flow is effectively 1D, while particle simulation is maintained to be fully 3D. Demixing becomes more pronounced [14] in such narrow beds.

In general, the gas phase variables in the last two terms in Eq. (3) are obtained by simultaneously integrating the balance equations for gas-solid mixtures; however, for the case of 1D incompressible gas phase, Eq. (3) can be simplified by considering the 1D continuity relation:

$$(1-\phi)\mathbf{u}_g + \phi \mathbf{u}_s = \mathbf{U}_s, \quad (4)$$

and the reduced momentum balance equation:

$$0 = -(1-\phi)\nabla p + \beta(\phi)(\mathbf{u}_s - \mathbf{u}_g), \quad (5)$$

where $\mathbf{u}_s$ is the coarse-grained particle velocity, and $\mathbf{U}_s$ is the superficial gas flow velocity, in the direction opposite to that of gravity. After some manipulation [using Eqs. (4) and (5)], Eq. (3) can be reduced as follows, where gas phase effects appear as additional terms in the individual equation of motion, involving solid phase coarse-grained, continuum variables:

$$m_p \frac{d\mathbf{v}_p}{dt} = m_p \mathbf{g} + \mathbf{F}_{\text{cont}} + \frac{V_p}{\phi}\beta(\phi) \times \left[(\mathbf{u}_s - \mathbf{v}_p) - \frac{1}{(1-\phi)^2}(\mathbf{u}_s - \mathbf{U}_s)\right]. \quad (6)$$

In our study, the Reynolds number based on the particle size is generally very small ($<\sim 0.1$), and β is approximated to be

$$\beta(\phi) = 18\frac{\mu_g}{d_p^2}\phi(1-\phi)^{-2.65}, \quad (7)$$

where μ_g is the gas phase viscosity. We nondimensionalize quantities by using ρ_s, d_p, $\sqrt{gd_p}$, and $\sqrt{d_p/g}$ as characteristic density, length, velocity, and time scales, where ρ_s is the solid phase mass density of the lighter particles. This detailed model accurately reproduces the minimum fluidization velocity, and has been used to study mechanically vibrated fluidized beds of cohesive fine powders [15].

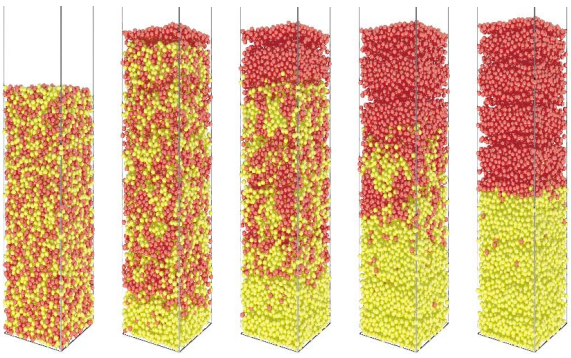

FIG. 1. (Color online) Snapshots of a gas-fluidized bed of a binary mixture of identical size but different density particles, undergoing spontaneous demixing, shown at times equally separated by $\Delta t=100$. Light-colored (yellow) particles are twice as dense as the dark-colored (red) ones ($e=0.9$; $\mu=0.1$; $k_n=2.0\times10^5$; $U_s=0.41$; $d_p=100$ μm; $\rho_s=0.90$ g/cm^3).

III. DIRECT SIMULATIONS

Demixing is typically a slow process, whose occurrence and duration depend on the density difference and the gas flow rate. Direct simulation (i.e., "brute-force" integration of the detailed model) with a sufficiently large U_s ($\equiv|\mathbf{U}_s|$), starting from a homogeneously mixed, packed (static) state (Fig. 1), shows that particles of different densities gradually demix spontaneously. When U_s is well above the minimum fluidization rate of both species (as in Fig. 1), a void region rises up in a periodic manner and the bed exhibits effectively 1D traveling waves (1D-TWs) [16]. Such waves are experimentally observed in narrow fluidized beds [17]. At these relatively large gas flow rates, demixing occurs superposed

on the persistent oscillatory motion driven by 1D-TWs.

A typical computation of an entire demixing process in the above "tiny" system (2×10^7 integration steps of 12 500 particles shown in Fig. 1) takes nearly two days (or more than a week for smaller gas flow rates, where demixing occurs even more slowly), on a single-processor PC of 1.7 GHz CPU. Obtaining an ensemble of long simulations for statistical averaging purposes can be extremely time-consuming even for such a small system.

Coarse-grained description and "observables"

In the literature, the degree of mixing or demixing is often characterized by various spatially lumped indices (or scalar "order parameters") [3,18–20] such as the so-called Lacey mixing index [18] (see its use, e.g., in Ref. [11]):

$$M = \frac{S_0^2 - S^2}{S_0^2 - S_R^2}, \tag{8}$$

where S_0 and S_R represent the variances for a completely demixed (segregated) and a completely mixed state, respectively, and S represents the variance for the (current snapshot of the) mixture between fully random and completely segregated states. Such an index provides convenient quantification; however, it does not suffice to describe the bed at a detailed level. In our study, we seek coarse-grained variables (or "observables") that could be useful in continuum modeling descriptions.

As in the two-fluid modeling approach [1], it is natural to think of hydrodynamic variables as candidate coarse observables. From computational experiments through direct simulation, we observe that, in the course of demixing in quasi-1D beds, the process depends nearly exclusively on the local density; this suggests that the *1D volume fraction profiles* themselves would be useful coarse observables. When, without disturbing the particle positions, we suddenly randomize the individual particle velocities (hence the granular temperature as well) and continue the simulation, the demixing process remains essentially undisturbed.

We recognize that the *cumulative distribution functions* (CDFs) of the particle positions,

$$F(h) = \int_0^h f(z)dz, \tag{9}$$

while effectively containing the same information as volume fraction profiles, are a slightly more convenient set of coarse observables; $f(z)$ above is the one-dimensional probability distribution function for particles' vertical positions (which can be thought of simply as a normalized volume fraction profile), and h is the specific bed height under consideration. Cumulative distribution functions, compared to volume fraction profiles, have the advantage of being smoother; they suffer from less noise, and they facilitate the *lifting* procedure (which will be explained below in Sec. IV A), an essential step in "equation-free" computations. As the CDFs are always bounded by 0 and 1, we choose their inverse, as our even more convenient coarse-grained variables in the following computations (Fig. 2). For these reasons we choose, instead of discretized volume fraction profiles (but equivalent to them), discretized inverse CDFs (ICDFs) as our actual coarse observables in the following. In traditional mathematical modeling, once the appropriate variables (coarse observables, here particle position ICDFs) are identified, one attempts to derive governing equations for their time evolution. Here, we follow instead an *equation-free* approach: We *circumvent* the derivation of such coarse-grained equations, yet still exploit their conceptual existence in accelerating detailed computation.

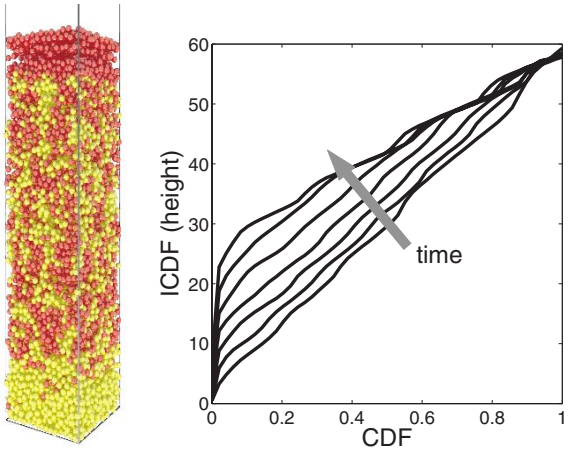

FIG. 2. (Color online) (Left panel) Snapshot of the bed at $t=150$ in Fig. 1. (Right panel) Time evolution of inverse CDFs (ICDFs) of the distribution of lighter particles (dark-colored; red in color online). Each line is separated by $\Delta t=50$, started from a fully mixed, fully fluidized state.

IV. EQUATION-FREE COMPUTATIONS

When time series of coarse-grained observables (obtained by short bursts of direct integration of the detailed model) are smooth and slowly varying, we can easily estimate their local time derivatives—not at the level of individual particle evolution, but—at the coarse-grained level of ICDF evolution. We can then *project* the system state (the ICDF profiles) to a future time (e.g., using the time derivative *estimates* in a forward Euler or more sophisticated scheme). If we now initialize the microscopic simulator consistent with the future (projected) values of the coarse observables, it is easy to see that we can actually accelerate the overall computation by "skipping" the integration of the detailed model over the projection time. This simple idea underpins *coarse projective integration* [21,22]; see Fig. 3 for illustration and below for details.

In equation-free computations, traditional continuum numerical techniques are directly applied to the outcome of appropriately initialized short bursts of microscopic (detailed) simulation, and the unavailable coarse-grained equations are "integrated" or "solved" without ever being written down [6,7,23]. The essential steps are the following:

(1) Identify coarse observables (which are discretized ICDFs or their parametrization coefficients in our study). For convenience, we denote the microscopic description (here

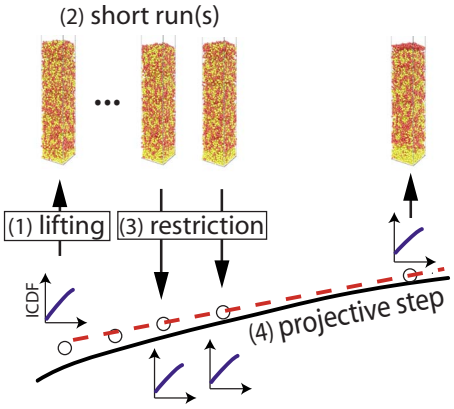

FIG. 3. (Color online) An illustration of coarse projective integration for demixing. Starting from a coarse-grained initial condition (the first circle, representing an instantaneous ICDF), (1) the detailed model is appropriately initialized (through lifting) and (2) integrated for a short time, during which (3) a series of ICDFs are recorded (through restriction). By making use of temporal smoothness of ICDF evolution, (4) a local temporal slope is estimated (solid straight line), and an ICDF at a significantly later future time is projected (dashed line); the whole procedure is repeated in time. The solid line represents ICDF evolution from a full-time detailed MD-based simulation.

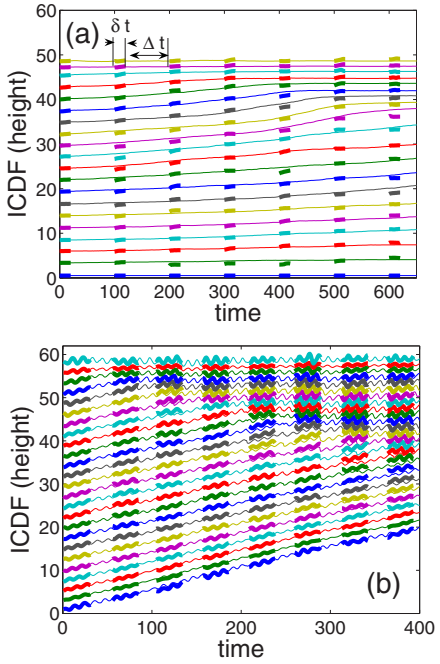

FIG. 4. (Color online) Direct, full integration (thin lines) and coarse projective integration (patches of thick lines), using an even discretization of the particle ICDFs as the coarse observables. (a) Slow demixing at $U_s=0.19$, where the bed hardly expands and no 1D-TWs form. Projective steps of $\Delta t=80$ were taken through forward Euler, after direct integration for $\delta t=20$ (the latter half of data were used to estimate the local slope). (b) In the presence of 1D-TWs ($U_s=0.41$), $\delta t=30$ and $\Delta t=2T$, where T is the average period estimated during short bursts of direct integrations; the last two periods of the locally oscillating data were used to estimate the coarse slope.

the individual particle positions) by $\mathbf{x}$, and their coarse-grained description (here the ICDFs) by $\mathbf{X}$.

(2) Choose an appropriate *lifting* operator μ_L, which maps $\mathbf{X}$ (ICDFs) to one (or more, for the purposes of variance reduction and ensemble-averaging) consistent description(s) $\mathbf{x}$ (here, particle positions). Figuring out an efficient lifting operator is essential.

(3) Using the lifting operator, initialize the detailed model consistent with desired coarse-grained values $\mathbf{x}(t_0)=\mu_L(\mathbf{X}(t_0))$.

(4) Run the detailed simulator for a short time horizon ($T_h>0$) to obtain $\mathbf{x}(t_0+T_h)$.

(5) Use an appropriate *restriction* operator $\mathcal{M}_R$ which maps the microscopic state(s) to the macroscopic description $\mathbf{X}(t_0+T_h)=\mathcal{M}_R(\mathbf{x}(t_0+T_h))$. This constitutes the coarse time-stepper Φ_{T_h} for the coarse observables: $\mathbf{X}(t_0+T_h)\equiv\Phi_{T_h}(\mathbf{X}(t_0))$. This process results in time series of the coarse observables (ICDFs).

(6) Apply desired numerical techniques (forward Euler, in our study) to the coarsely observed results in step (4), and repeat, so as to accelerate the overall simulation.

A. From ICDFs to consistent particle configurations: Lifting

In the lifting step, given an ICDF as the coarse observable, we need to be able to efficiently construct particle configurations consistent with it. Arranging particles (i.e., sphere packing) in *three-dimensional* space with an *arbitrarily* prescribed volume fraction profile, especially when dense, is nontrivial and generally time-consuming [24], as excessive particle-particle overlap has to be avoided; it would be less difficult for dilute particulate flows. In our study, the total height of a bed remains virtually the same, even in the presence of 1D-TWs (see the second and later frames in Fig. 1). We do not, therefore, reassign particle positions from scratch in each lifting step. Instead, we utilize particle locations available from an earlier step, and switch *only* particle indices (or "colors," whether "red" or "yellow") until the prescribed ICDF becomes satisfied; this makes the lifting operator computationally inexpensive. For *polydisperse* particles this scheme is clearly insufficient, and should be modified; this would be a subject of future research.

For a narrow range of U_s's slightly above the minimum fluidization rate, the time evolution of ICDFs does not exhibit any waviness [see thin lines in Fig. 4(a) and Sec. IV B], and demixing occurs very slowly (complete demixing is hardly achieved). In this case, discretized ICDFs or their compact parametric representation (see Sec. IV C) can be used as actual coarse observables for the lifting and projection, in a straightforward manner; particle positions from a "snapshot" of the bed at any time can be used for the lifting at a later time.

At larger U_s's, ICDFs locally oscillate at a fast time scale [see Figs. 2 and 4(b) and Sec. IV B]. Our lifting operator for single realization computations of such a case requires additional consideration, as 1D-TWs are present: We therefore use particle locations obtained at the *same* "phase angle" of the wave propagation in earlier simulations. In ensemble-averaged computations, this oscillatory feature of the bed

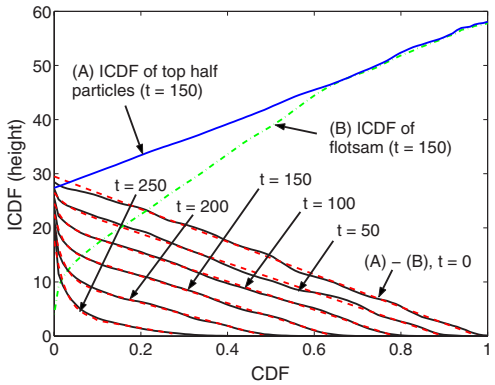

FIG. 5. (Color online) Evolving inverse CDFs (ICDFs) for the same case as in Fig. 1, averaged over 10 realizations: (A) ICDF of particles physically located in the upper half of the bed and (B) ICDF of the lighter particles, which are shown at $t=150$. Solid lines with negative slopes are snapshots of the difference between (A) and (B) at different times; compare with the functional fit shown as dashed lines; see Eq. (10).

becomes smoothed through averaging (over various phase angles during the oscillations), requiring no special attention (Sec. IV C).

B. Coarse projective integration using discretized ICDFs

We begin by choosing discretized ICDFs of the lighter particles as the coarse observables. We accelerate the demixing computation using the coarse projective forward Euler scheme [21,22]. For smaller U_s (slightly above the minimum fluidization rate), where the bed hardly expands and ICDFs do not oscillate, the projection step size is determined by only the temporal smoothness (accuracy of the local linearization) of ICDF evolution. The demixing occurs very slowly in this case [Fig. 4(a)], and coarse projective integration can achieve high computational speedup. When excessively large projection step sizes are chosen, they can cause inaccuracies, similar to large time steps in normal numerical integration of ordinary differential equations. For larger values of U_s, in the presence of 1D-TWs the projection step size is chosen to be an integral multiple of the local oscillation period [Fig. 4(b)]. Lifting in both cases requires only negligible extra cost, and the computational gain realized by the coarse projective integration is determined by the ratio betweeen the short burst duration (required to accurately estimate the time derivative) and the projective step size. In Fig. 4 the computational gain factor observed ranges between two and five (we observed gain factors up to about ten in other cases).

Projectively integrated values (thick lines in Fig. 4) follow the trajectories of direct, full integrations (thin lines in Fig. 4) well, validating our choice of coarse observables. These are indeed the variables that one should use to obtain closed-form coarse-grained equations. Ensemble-averaging of ICDFs over different realizations (of different phase angles during wave propagation) smoothens local oscillations arising from 1D-TWs. Projective integration of ensemble-averaged ICDFs, both in the presence and absence of 1D-TWs, can be applied in the same way as was done for the case shown in Fig. 4(a); no extra consideration is necessary, even when 1D-TWs are present.

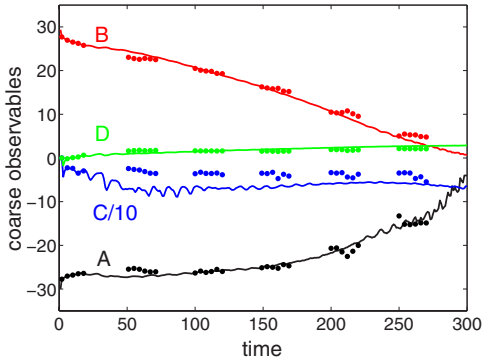

FIG. 6. (Color online) Comparison between direct, full integrations (solid lines) and coarse projective integrations (groups of dots), using the four coarse observables in Eq. (10).

C. A more compact description

The difference between the ICDF of particles located in the *upper half* of the bed (irrespective of their densities) and that of the lighter ones can serve as a useful alternative coarse observable. Indeed, the ICDFs of the lighter particles are bounded by those of the (total) top half particles, and hence their difference is always positive definite (Fig. 5). Furthermore, once nearly-full local demixing occurs, the ICDF difference there becomes virtually zero. The difference of the two ICDFs can be fit by the following simple functional form, quantifiable with only four variables (dashed lines in Fig. 5):

$$y = \max[Ax + B + C\exp(Dx), 0], \tag{10}$$

where $A(t)$, $B(t)$, $C(t)$, and $D(t)$ (parametric representation of the functional shape) are our new coarse observables; x and y represent the abscissa and the ordinate in Fig. 5, respectively. During a detailed simulation the values of these observables (restriction) are determined on the fly by functional fitting. Other basis functions, such as high-order polynomials also can fit the functional form reasonably well, but they require many more terms (due to large curvatures for small values of CDFs at later times). Furthermore, the time evolution of higher order coefficients of such an expansion may not be (and we observed it not to be) slow. The lifting procedure using these new coarse observables involves a minor intermediate step, compared to the ones in Sec. IV B; a mapping between these four variables and an ICDF discretization through the functional form in Eq. (10).

We use these four coarse observables to perform ensemble-averaged coarse projective integration over a number of realizations (Fig. 6). These observables vary slowly and smoothly in time (occasional oscillations disappear for larger ensembles); in a sense, this is a pseudospectral solution of the unknown governing equations for ICDF evolution.

V. CONCLUSIONS

We have used an equation-free coarse-grained approach to accelerate (by a factor of two to ten; the lifting step in our study involves minimal computational cost) detailed computations of dense particulate flows and, in particular, of demixing occurring in gas-fluidized beds of particle mixtures of dissimilar density. This approach holds promise for the accelerated prediction of coarse-grained behavior at practically relevant spatial and temporal scales. Note that here we coarse-grained originally $\sim 10N$-dimensional detailed model eventually down to four-dimensional coarse-grained description (Sec. IV C), where N is the number of particles ($\sim 10\,000$).

We deliberately considered a quasi-1D illustrative problem in our study, in order to demonstrate the viability of the approach. As a consequence of the problem considered in this study, the coarse observables were *one-dimensional* discretized ICDFs or their parametric representations. For systems involving higher dimensional flows, candidates for coarse observables include marginal and conditional ICDFs [25]. More work for such systems has to be done to identify proper coarse observables and an efficient lifting operator, vital components of the approach. Ensemble averaging reduces fluctuations among the realizations, giving better quantitative statistical representations. One can easily see that the computation of each realization can be readily parallelized across computational nodes.

More sophisticated equation-free algorithms that we have not used here (e.g., coarse fixed point algorithms [6]) can be applied to find stable as well as unstable steady states; quantify their stability; and perform numerical bifurcation analysis. Exploiting such tools to investigate the coarse-grained dynamics of mixing and demixing (and other particulate flow problems) is the subject of current research.

ACKNOWLEDGMENTS

This research was partially supported by DOE, DARPA, and ACS-PRF.

[1] R. Jackson, *The Dynamics of Fluidized Particles* (Cambridge University Press, Cambridge, UK, 2000); S. Sundaresan, Annu. Rev. Fluid Mech. **35**, 63 (2003).
[2] I. Goldhirsh, Annu. Rev. Fluid Mech. **35**, 267 (2003).
[3] P. N. Rowe, A. W. Nienow, and A. J. Agbim, Trans. Inst. Chem. Eng. **50**, 310 (1972); A. W. Nienow, P. N. Rowe, and L. Y.-L. Cheung, Powder Technol. **20**, 89 (1978).
[4] L. G. Gibilaro and P. N. Rowe, Chem. Eng. Sci. **29**, 1403 (1974).
[5] B. G. van Wachem, J. C. Schouten, C. M. van den Bleek, R. Krishna, and J. L. Sinclair, AIChE J. **47**, 1292 (2001).
[6] I. G. Kevrekidis *et al.*, Commun. Math. Sci. **1**, 715 (2003).
[7] I. G. Kevrekidis, C. W. Gear, and G. Hummer, AIChE J. **50**, 1346 (2004).
[8] P. A. Cundall and O. D. L. Strack, Geotechnique **29**, 47 (1979).
[9] Y. Tsuji, T. Kawaguchi, and T. Tanaka, Powder Technol. **77**, 79 (1993).
[10] B. P. B. Hoomans *et al.*, Chem. Eng. Sci. **51**, 99 (1996); B. P. B. Hoomans, J. A. M. Kuipers, and W. P. M. Van Swaaij, Powder Technol. **109**, 41 (2000).
[11] Y. Q. Feng, B. H. Xu, S. J. Zhang, A. B. Yu, and P. Zulli, AIChE J. **50**, 1713 (2004).
[12] *Fluidization*, 2nd ed., edited by J. F. Davidson, R. Clift, and D. Harrison (Academic Press, London, 1985).
[13] C. Y. Wen and Y. H. Yu, Chem. Eng. Prog., Symp. Ser. **62**, 100 (1966).
[14] B. Formisani, G. De. Cristofaro, and R. Girimonte, Chem. Eng. Sci. **56**, 109 (2001).
[15] S. J. Moon, I. G. Kevrekidis, and S. Sundaresan, Ind. Eng. Chem. Res. **45**, 6966 (2006).
[16] S. J. Moon, I. G. Kevrekidis, and S. Sundaresan, Phys. Fluids **18**, 083304 (2006).
[17] P. Duru, M. Nicolas, E. J. Hinch, and É. Guazzelli, J. Fluid Mech. **452**, 371 (2002).
[18] P. M. C. Lacey, J. Appl. Chem. **4**, 257 (1954).
[19] R. W. Rice and J. F. Brainovich, AIChE J. **32**, 35 (1986).
[20] A. W. Nienow, N. S. Naimer, and T. Chiba, Chem. Eng. Commun. **62**, 53 (1987).
[21] C. W. Gear, I. G. Kevrekidis, and C. Theodoropoulos, Comput. Chem. Eng. **26**, 941 (2002).
[22] C. W. Gear and I. G. Kevrekidis, SIAM J. Sci. Comput. (USA) **24**, 1091 (2003).
[23] C. Theodoropoulos, Y. H. Qian, and I. G. Kevrekidis, Proc. Natl. Acad. Sci. U.S.A. **97**, 9840 (2000).
[24] S. Torquato, *Random Heterogeneous Materials: Microstructure and Macroscopic Properties* (Springer-Verlag, New York, 2002).
[25] Y. Zou, I. G. Kevrekidis, and R. Ghanem, Phys. Rev. E **72**, 046702 (2005).